903. Free vibration studies of functionally graded magneto-electro-elastic plates/shells by using solid-shell elements

Zheng Shijie[1], Fen Yan[2], Wang Hongtao[3]
[1, 2]State Key Laboratory of Mechanics and Control of Mechanical Structures
Nanjing University of Aeronautics and Astronautics, Nanjing, 210016, China
[3]School of Mechanical and Electrical Engineering
Nanjing University of Aeronautics and Astronautics, Nanjing 210016, China
E-mail: [1]*sjzheng@nuaa.edu.cn*, [3]*xwwang@nuaa.edu.cn*, [3]*meehtwang@nuaa.edu.cn*

(Received 23 September 2012; accepted 4 December 2012)

Abstract. In this article, free vibration studies on functionally graded magneto-electro-elastic plates and cylindrical shells have been carried out by means of finite element method. The functionally graded material is assumed to be exponential in the thickness direction. The present finite element is formulated on the basis of assumed natural strain, enhanced assumed strain method and using displacement components, electric potential and magnetic potentials as nodal degrees of freedom. This element can be used as solid element and can also be applied to model thin curved shell structures. Numerical studies include the influence of the different exponential factor, magnetic and piezoelectric effect on the natural frequencies. Obtained numerical results are in good agreement with the semi-analytical finite element solutions available in the literature.

Keywords: functionally graded materials, magneto-electro-elastic, free vibration, finite element, plates/shells.

1. Introduction

Smart or intelligent materials such as the piezoelectric and piezomagnetic ones have attracted considerable interest recently due to their ability of converting energy from one type to the other (among magnetic, electric and mechanical energies). Magneto-electro-elastic materials simultaneously possess piezoelectric, piezomagnetic and magneto-electro-elastic effects, which is two orders higher than that of the individual constituent materials. With application in ultrasonic imaging devices, sensors, actuators, transducers and many other emerging components, there is a strong need for theories or techniques that can predict the coupled response of these smart materials as well as structure composed of them. Studies on static and dynamic behavior on simply supported plates as well as cylindrical shells have been dealt in literature [1-9].

In recent years, functionally graded (FG) materials, a novel microscopically inhomogeneous composites usually made from a mixture of metals and ceramics with continuously varying volume fractions of two materials along the thickness direction, have gained big attention in engineering community. But the studies on non-homogeneous magneto-electro-elastic structure are relatively scarce. Cao, Shi and Jin [10] employed the power series technique for solving the propagation behavior of Lamb waves in the FG piezoelectric-piezomagnetic material plate with material parameters varying continuously along the thickness direction. Wu and Tsai [11] used the method of perturbation to present a three-dimensional (3D) free vibration analysis of simply supported, doubly-curved FG magneto-electro-elastic shells with closed-circuit surface conditions. Pan and Han [12] presented an exact solution for FG and layered magneto-electro-elastic plates by pseudo-Stroh formalism. Huang, Ding and Chen [13] derived the analytical and semi-analytical solutions for anisotropic FG magneto-electro-elastic beams

subjected to an arbitrary load, which can be expanded in terms of sinusoidal series. Their analysis is applicable to beams with various boundary conditions at the two ends. Free vibration analysis of FGM and layered magneto-electro-elastic plates has been carried out by using series solution in conjunction with finite element approach [14].

From the literature survey, it is found that only several studies have been reported on magneto-electro-elastic structures analyzed by semi-analytical finite element analysis. To the author's knowledge there is no finite element formulation without combining with series solution available for vibration studies on FG magneto-electro-elastic plates and shells. Hence, in present study, a solid-shell element formulation is presented for the free vibration analysis of FG magneto-electro-elastic plates and shells by using enhanced assumed strain and assumed natural strain methods. For the study, magneto-electro-elastic material made of a homogenous mixture of piezoelectric barium titanate ($BaTiO_3$) as the embedded material and piezomagnetic cobalt ferrite ($CoFe_2O_4$) as the matrix material is considered.

2. Constitutive equations

2.1. Governing equation

For anisotropic and linearly magneto-electro-elastic solid the coupled constitutive equations for a general three-dimensional solid is as follows [1]:

$$\begin{aligned} \sigma_j &= C_{jk} S_k - e_{kj} E_k - q_{kj} H_k \\ D_j &= e_{jk} S_k + \varepsilon_{jk} E_k + m_{jk} H_k, \\ B_j &= q_{jk} S_k + m_{jk} E_k + \mu_{jk} H_k \end{aligned} \tag{1}$$

where σ_j, D_j and B_j indicate the stress, electric displacement and magnetic induction. S_k, E_k and H_k are strain, electric field and magnetic field, respectively. C_{jk}, ε_{jk} and μ_{jk} are the elastic, dielectric and magnetic permeability coefficients, respectively. e_{kj}, q_{kj} and m_{jk} are the piezoelectric, piezomagnetic and magneto-electro-elastic material coefficients, respectively. A completely coupled magneto-electro-elastic material matrix, assuming a hexagonal crystal class, for above constitutive equations is given by Buchanan [7].

The present study considers FG material composed of piezoelectric and magnetostrictive material. The grading is accounted across the thickness of the shell. This has been achieved by grading the volume fraction distribution of either piezoelectric or magnetostrictive material governed by a simple power-law exponent.

In the present case, a simple power-law-type definition for the volume fraction of $BaTiO_3$ across the thickness direction of the FGM plate is defined as:

$$V_B = \left(\frac{2z + h}{2h} \right)^n, \tag{2}$$

where h - thickness of the plate, z - thickness coordinates ($0 \le z \le h$), and n - power-law index. The bottom surface of the plate ($0 \le z \le h$) is $CoFe_2O_4$-rich, whereas the top surface ($0 \le z \le h$) of the plate is $BaTiO_3$-rich, and the sum of the total volume fractions of the constituent materials, $BaTiO_3$ (B) and $CoFe_2O_4$ (F) should be one.

While in the case of an FGM cylindrical shell, the volume fraction of $CoFe_2O_4$(F) across the radial direction of the shell is assumed as:

© VIBROENGINEERING. JOURNAL OF VIBROENGINEERING. DECEMBER 2012. VOLUME 14, ISSUE 4. ISSN 1392-8716

$$V_F = \left(\frac{r_z - r_i}{r_o - r_i} \right)^n, \tag{3}$$

where r_z represents radius at any point along the radial direction of the shell, r_i is the inner radius, r_o is the outer radius of the shell. Based on the above definition it follows that the inner surface of the cylindrical shell will be piezo-rich.

On the basis of the volume fraction definition and law of mixtures, the effective material property definition follows:

$$P_{eff}(\varsigma_3) = \sum_{j=1} P_j V_j(\varsigma_3), \tag{4}$$

where P_j and V_j are material properties and volume fraction of the constituent material j comprising the functionally graded material. 'P_{eff}' is general notation for material property. Making use of equation (2)-(4) the effective elastic, piezoelectric, piezomagnetic, dielectric and magnetic permeability definitions can be derived.

3. Finite element formulation

In this section, the eight-node magneto-electro-elastic solid shell element is described. The element has four nodes at each of its top ($\zeta = 1$) and bottom faces ($\zeta = -1$). The mapping between the global Cartesian co-ordinates (X, Y, Z) and the natural coordinates (ξ, η, ζ) is:

$$\begin{aligned} \boldsymbol{X}(\xi,\eta,\zeta) &= \sum_{i=1}^{4} \boldsymbol{N}_i(\xi,\eta)(\zeta^+ X_i + \zeta^- X_{4+i}) = \boldsymbol{N}_0(\xi,\eta)\boldsymbol{X}_e + \zeta \boldsymbol{N}_n(\xi,\eta)\boldsymbol{X}_e, \\ \boldsymbol{U}(\xi,\eta,\zeta) &= \sum_{i=1}^{4} \boldsymbol{N}_i(\xi,\eta)(\zeta^+ U_i + \zeta^- U_{4+i}) = \boldsymbol{N}_0(\xi,\eta)\boldsymbol{U}_e + \zeta \boldsymbol{N}_n(\xi,\eta)\boldsymbol{U}_e, \end{aligned} \tag{5}$$

where $N_i's$ are the two-dimensional Lagrangian interpolation functions,

$$\begin{aligned} \boldsymbol{N}_0 &= \tfrac{1}{2}\left[N_1\boldsymbol{I}_3 \quad \cdots \quad N_4\boldsymbol{I}_3 \quad N_1\boldsymbol{I}_3 \quad \cdots \quad N_4\boldsymbol{I}_3 \right], \\ \boldsymbol{N}_n &= \tfrac{1}{2}\left[N_1\boldsymbol{I}_3 \quad \cdots \quad N_4\boldsymbol{I}_3 \quad -N_1\boldsymbol{I}_3 \quad \cdots \quad -N_4\boldsymbol{I}_3 \right], \end{aligned} \tag{6}$$

$$\begin{aligned} \boldsymbol{X}_e &= \left\{ X_1 \quad Y_1 \quad Z_1 \quad \ldots \quad X_8 \quad Y_8 \quad Z_8 \right\}^T, \\ \boldsymbol{U}_e &= \left\{ U_1 \quad V_1 \quad W_1 \quad \ldots \quad U_8 \quad V_8 \quad W_8 \right\}^T. \end{aligned} \tag{7}$$

Here, the strain-displacement relation of the element will be presented. With reference to the interpolations of $\boldsymbol{X}$ and $\boldsymbol{U}$, the strain with respect to (ξ, η, ζ) is computed, i.e.:

$$\begin{aligned} &S_\xi = \boldsymbol{X}_{,\xi}^T \boldsymbol{U}_{,\xi}, \quad S_\eta = \boldsymbol{X}_{,\eta}^T \boldsymbol{U}_{,\eta}, \quad S_\zeta = \boldsymbol{X}_{,\zeta}^T \boldsymbol{U}_{,\zeta}, \\ &S_{\xi\eta} = \boldsymbol{X}_{,\xi}^T \boldsymbol{U}_{,\eta} + \boldsymbol{X}_{,\eta}^T \boldsymbol{U}_{,\xi}, \quad S_{\zeta\xi} = \boldsymbol{X}_{,\zeta}^T \boldsymbol{U}_{,\xi} + \boldsymbol{X}_{,\xi}^T \boldsymbol{U}_{,\zeta}, \quad S_{\zeta\eta} = \boldsymbol{X}_{,\zeta}^T \boldsymbol{U}_{,\eta} + \boldsymbol{X}_{,\eta}^T \boldsymbol{U}_{,\zeta}. \end{aligned} \tag{8}$$

It has been rather standard practice to use an assumed natural strain (ANS) method for resolving the shear locking and trapezoidal locking. Shear locking is due to the excess number of transverse shear strains sampled in the process of integrating the element stiffness matrix.

The ANS method is an effective method of resolving shear locking. By using ANS method, the number of independent shear strains in the system level can be reduced. The natural transverse shear strains are modified to be [15, 16]:

$$\begin{aligned}\tilde{S}_{\zeta\xi}&=\frac{1-\eta}{2}S_{\zeta\xi}^{\xi=0,\eta=-1}+\frac{1+\eta}{2}S_{\zeta\xi}^{\xi=0,\eta=+1},\\ \tilde{S}_{\zeta\xi}&=\frac{1-\xi}{2}S_{\zeta\eta}^{\xi=-1,\eta=0}+\frac{1+\xi}{2}S_{\zeta\eta}^{\xi=+1,\eta=0}.\end{aligned} \tag{9}$$

Similar to shear locking, the excessive number of sampled thickness strains lead to trapezoidal locking. Trapezoidal locking occurs when the common shell element is used to model curved shells. It can also be reduced in the system level by sampling the strain along the element edges, i.e. [15, 16]:

$$\tilde{S}_{\zeta}=N_1\tilde{S}_{\zeta}^{\xi=-1,\eta=-1}+N_2\tilde{S}_{\zeta}^{\xi=+1,\eta=-1}+N_3\tilde{S}_{\zeta}^{\xi=+1,\eta=+1}+N_4\tilde{S}_{\zeta}^{\xi=-1,\eta=+1}. \tag{10}$$

The conventional eight-node solid elements have a significant deficiency when the element thickness is small compared with the element span, the excessive shear strain energy stored in the thickness direction will lead to a much higher stiffness coefficient than those in planar directions. To overcome the thickness locking of solid shell elements, a linear extension EAS over the thickness is used to enhance the strain in the thickness direction [16]:

$$\begin{aligned}&\overline{S}_{\zeta}=S_{\zeta}+\zeta\Delta S_{\zeta}^{EAS},\\ &\Delta S_{\zeta}^{EAS}=\frac{1}{|\boldsymbol{J}|}\begin{bmatrix}1 & \xi & \eta & \xi\eta\end{bmatrix}\boldsymbol{\Delta\lambda}=\boldsymbol{B}_{\zeta}^{EAS}\boldsymbol{\Delta\lambda},\\ &\boldsymbol{\Delta\lambda}=\begin{Bmatrix}\lambda_1 & \lambda_2 & \lambda_3 & \lambda_4\end{Bmatrix}^T,\end{aligned} \tag{11}$$

where $|\boldsymbol{J}|$ is the value of the determinant of the Jacobian.

As the material properties are often defined in a local orthogonal frame (x, y, z), it is necessary to obtain the local physical strains from the ones with respect to (ξ, η, ζ). It will be assumed that z-axis is perpendicular to the mid-surface of the shell. Hence the relation between the nature coordinate infinitesimal strains and the local physical strains is:

$$\boldsymbol{S}=\boldsymbol{T}\begin{Bmatrix}S_{\xi} & S_{\eta} & \tilde{S}_{\zeta}+\zeta\Delta S_{z}^{EAS} & \tilde{S}_{\zeta\eta} & \tilde{S}_{\zeta\xi} & S_{\xi\eta}\end{Bmatrix}=\boldsymbol{B}_u\boldsymbol{U}_e, \tag{12}$$

where $\boldsymbol{T}$ is the strain transformation matrix [16].

For eight-node magneto-electro-elastic solid shell element with one electric degree and magnetic degree per node, the electrical potential field and the magnetic field are adopted as follows:

$$\boldsymbol{E}=-\boldsymbol{B}_{\phi}\boldsymbol{\varphi}_e,\ \boldsymbol{H}=-\boldsymbol{B}_{\psi}\boldsymbol{\psi}_e, \tag{13}$$

$$\boldsymbol{B}_{\phi}=\boldsymbol{T}_{\phi}\begin{bmatrix}\boldsymbol{N}_{\phi,\xi}\\ \boldsymbol{N}_{\phi,\eta}\\ \boldsymbol{N}_{\phi,\zeta}\end{bmatrix},\ \boldsymbol{B}_{\psi}=\boldsymbol{T}_{\psi}\begin{bmatrix}\boldsymbol{N}_{\psi,\xi}\\ \boldsymbol{N}_{\psi,\eta}\\ \boldsymbol{N}_{\psi,\zeta}\end{bmatrix}, \tag{14}$$

© VIBROENGINEERING. JOURNAL OF VIBROENGINEERING. DECEMBER 2012. VOLUME 14, ISSUE 4. ISSN 1392-8716

$$\boldsymbol{N}_{\phi} = \left[\underline{N}_1 \quad \cdots \quad \underline{N}_8\right],\ \boldsymbol{N}_{\psi} = \left[\underline{N}_1 \quad \cdots \quad \underline{N}_8\right], \tag{15}$$

where $\underline{N}_i's$ are the three-dimensional Lagrangian interpolation functions, $\boldsymbol{T}_{\phi}$, $\boldsymbol{T}_{\psi}$ is the transformation matrix.

The thermodynamic potential for a 3-D magneto-electro-elastic solid is given by:

$$\boldsymbol{G} = \boldsymbol{G}\left(\boldsymbol{S}, \boldsymbol{E}, \boldsymbol{H}\right), \tag{16}$$

where $\boldsymbol{S}$, $\boldsymbol{E}$ and $\boldsymbol{H}$ are independent variables which represent strain, electric field and magnetic field, respectively. By using Eq. (1) in Eq. (16), the variation expression for magneto-electro-elastic solid can be obtained as follows:

$$\boldsymbol{G} = \left(\frac{1}{2}\boldsymbol{S}^{\boldsymbol{T}}\boldsymbol{C}\boldsymbol{S}\right) - \left(\frac{1}{2}\boldsymbol{E}^{\boldsymbol{T}}\boldsymbol{\varepsilon}\boldsymbol{E}\right) - \left(\frac{1}{2}\boldsymbol{H}^{\boldsymbol{T}}\boldsymbol{\mu}\boldsymbol{H}\right) - \boldsymbol{S}\boldsymbol{e}\boldsymbol{E} - \boldsymbol{S}\boldsymbol{q}\boldsymbol{H} - \boldsymbol{E}\boldsymbol{m}\boldsymbol{H}, \tag{17}$$

where $\boldsymbol{C}$, $\boldsymbol{\varepsilon}$, $\boldsymbol{\mu}$ represent elastic, dielectric and magnetic permeability coefficients and $\boldsymbol{e}$, $\boldsymbol{q}$, $\boldsymbol{m}$ indicate the piezoelectric, piezo-magnetic and magneto-electric coefficients, respectively.

By minimizing Eq. (17) for nodal variables of shape functions for strain-displacement, electric field-electric potential, and magnetic field-magnetic potential, the finite element equations for magneto-electro-elastic solid can be obtained. A formulation for such coupled field variables can be written as [2]:

$$\begin{aligned}
&\left(\boldsymbol{K}_{uu} - \omega^2\boldsymbol{M}\right)\boldsymbol{u} + \boldsymbol{K}_{u\phi}\boldsymbol{\varphi} + \boldsymbol{K}_{u\psi}\boldsymbol{\psi} = 0,\\
&\boldsymbol{K}_{u\phi}^{T}\boldsymbol{u} - \boldsymbol{K}_{\phi\phi}\boldsymbol{\varphi} - \boldsymbol{K}_{\phi\psi}\boldsymbol{\psi} = 0,\\
&\boldsymbol{K}_{u\psi}^{T}\boldsymbol{u} - \boldsymbol{K}_{\phi\psi}\boldsymbol{\varphi} - \boldsymbol{K}_{\psi\psi}\boldsymbol{\psi} = 0.
\end{aligned} \tag{18}$$

Various stiffness matrices are defined as follows:

$$\begin{aligned}
&\boldsymbol{K}_{uu} = \int_v \boldsymbol{B}_u^T\boldsymbol{C}\boldsymbol{B}_u dv,\quad \boldsymbol{K}_{u\phi} = \int_v \boldsymbol{B}_u^T\boldsymbol{e}\boldsymbol{B}_{\phi} dv,\\
&\boldsymbol{K}_{u\psi} = \int_v \boldsymbol{B}_u^T\boldsymbol{q}\boldsymbol{B}_{\boldsymbol{\varphi}} dv,\quad \boldsymbol{K}_{\phi\psi} = \int_v \boldsymbol{B}_{\phi}^T\boldsymbol{m}\boldsymbol{B}_{\psi} dv,\\
&\boldsymbol{K}_{\phi\phi} = \int_v \boldsymbol{B}_{\phi}^T\boldsymbol{\varepsilon}\boldsymbol{B}_{\phi} dv,\quad \boldsymbol{K}_{\psi\psi} = \int_v \boldsymbol{B}_{\psi}^T\mu\boldsymbol{B}_{\psi} dv.
\end{aligned} \tag{19}$$

$\boldsymbol{B}_u$, $\boldsymbol{B}_{\phi}$ and $\boldsymbol{B}_{\psi}$ denotes the strain-displacement, electric field-electric potential and magnetic field-magnetic potential relations, respectively.

Mass matrix for the structure is:

$$\boldsymbol{M} = \int \left(\boldsymbol{N}_0 + \zeta\boldsymbol{N}_n\right)^T \rho\left(\boldsymbol{N}_0 + \zeta\boldsymbol{N}_n\right) dv. \tag{20}$$

In equation (18) by using a condensation technique $\boldsymbol{\varphi}$ and $\boldsymbol{\psi}$ are eliminated to obtain an equivalent system stiffness matrix $\boldsymbol{K}_{eq}$. The equation of motion for the system can be written as:

$$\boldsymbol{M}\ddot{\boldsymbol{U}} + \boldsymbol{K}_{eq}\boldsymbol{U} = 0, \tag{21}$$

where:

$$\boldsymbol{K}_{eq} = \boldsymbol{K}_{uu} + \boldsymbol{K}_{u\phi}\boldsymbol{K}_{\mathrm{II}}^{-1}\boldsymbol{K}_{\mathrm{I}} + \boldsymbol{K}_{u\psi}\boldsymbol{K}_{\mathrm{IV}}^{-1}\boldsymbol{K}_{\mathrm{III}}. \tag{22}$$

The component matrices for Eq. (19) are:

$$\begin{aligned}
\boldsymbol{K}_{\mathrm{I}} &= \boldsymbol{K}_{u\phi}^{T} - \boldsymbol{K}_{\phi\psi}\boldsymbol{K}_{\psi\psi}^{-1}\boldsymbol{K}_{u\psi}^{T},\\
\boldsymbol{K}_{\mathrm{II}} &= \boldsymbol{K}_{\phi\phi} - \boldsymbol{K}_{\phi\psi}\boldsymbol{K}_{\psi\psi}^{-1}\boldsymbol{K}_{\phi\psi}^{T},\\
\boldsymbol{K}_{\mathrm{III}} &= \boldsymbol{K}_{u\psi}^{T} - \boldsymbol{K}_{\phi\psi}^{T}\boldsymbol{K}_{\phi\phi}^{-1}\boldsymbol{K}_{u\phi}^{T},\\
\boldsymbol{K}_{\mathrm{IV}} &= \boldsymbol{K}_{\psi\psi} - \boldsymbol{K}_{\phi\psi}^{T}\boldsymbol{K}_{\phi\phi}^{-1}\boldsymbol{K}_{\phi\psi}.
\end{aligned} \tag{23}$$

The eigenvectors that correspond to the distribution of $\boldsymbol{\varphi}$ and $\boldsymbol{\psi}$ are shown below:

$$\boldsymbol{\varphi} = \boldsymbol{K}_{II}^{-1}\boldsymbol{K}_{I}\boldsymbol{u}, \quad \boldsymbol{\psi} = \boldsymbol{K}_{IV}^{-1}\boldsymbol{K}_{III}\boldsymbol{u}. \tag{24}$$

To study the magneto-electric effect on the system frequencies, the equivalent stiffness matrix $\boldsymbol{K}_{eq\_reduced}$ is derived by neglecting the coupling between the piezoelectric $BaTiO_3$ and piezomagnetic $CoFe_2O_4$ materials. The magneto-electric material coefficient ($\boldsymbol{m}$) is zero for single phase $BaTiO_3$ and $CoFe_2O_4$. From equation (18), by putting $\boldsymbol{K}_{\varphi\psi}$ = 0, the reduced finite element equations are as follows:

$$\begin{aligned}
&\left(\boldsymbol{K}_{uu} - \omega^2\boldsymbol{M}\right)\boldsymbol{u} + \boldsymbol{K}_{u\phi}\boldsymbol{\varphi} + \boldsymbol{K}_{u\psi}\boldsymbol{\psi} = 0,\\
&\boldsymbol{K}_{u\phi}^{T}\boldsymbol{u} - \boldsymbol{K}_{\phi\phi}\boldsymbol{\varphi} = 0,\\
&\boldsymbol{K}_{u\psi}^{T}\boldsymbol{u} - \boldsymbol{K}_{\psi\psi}\boldsymbol{\psi} = 0.
\end{aligned} \tag{25}$$

The reduced stiffness matrix $\boldsymbol{K}_{eq\_reduced}$ is shown below:

$$\boldsymbol{K}_{eq\_reduced} = \boldsymbol{K}_{uu} + \boldsymbol{K}_{u\phi}\boldsymbol{K}_{\phi\phi}^{-1}\boldsymbol{K}_{u\phi}^{T} + \boldsymbol{K}_{u\psi}\boldsymbol{K}_{\psi\psi}^{-1}\boldsymbol{K}_{u\psi}^{T}. \tag{26}$$

To study the piezoelectric effect due to piezoelectric $BaTiO_3$ on the frequency of the magneto-electro-elastic structures, the stiffness matrix $\boldsymbol{K}_{eq\_\phi\phi}$ is derived by putting magnetic potential to zero as follows:

$$\boldsymbol{K}_{eq\_\phi\phi} = \boldsymbol{K}_{uu} - \boldsymbol{K}_{u\phi}\boldsymbol{K}_{\phi\phi}^{-1}\boldsymbol{K}_{u\phi}^{T}. \tag{27}$$

To study the magnetic effect of piezomagnetic $CoFe_2O_4$ on the frequency of the system, $\boldsymbol{K}_{eq\_\psi\psi}$ is used as the stiffness matrix and is expressed as:

$$\boldsymbol{K}_{eq\_\psi\psi} = \boldsymbol{K}_{uu} + \boldsymbol{K}_{u\psi}\boldsymbol{K}_{\psi\psi}^{-1}\boldsymbol{K}_{u\psi}^{T}. \tag{28}$$

4. Results and discussion

In this section, we present some numerical results by using the finite element formulation proposed in this paper. Plate and shell problems are considered for validating the presented finite element method. Material constants are given in several papers and Aboudi [17] is the source for the material parameters used here and hence not repeated here. The density of $BaTiO_3$ and $CoFe_2O_4$ is assumed to be the same 5730 kg/m^3. $f_{uu}, f_{eq}, f_{eq\_reduce}, f_{\psi\psi}$ and $f_{\phi\phi}$

© VIBROENGINEERING. JOURNAL OF VIBROENGINEERING. DECEMBER 2012. VOLUME 14, ISSUE 4. ISSN 1392-8716

are system frequencies, which are computed by using $\boldsymbol{K}_{uu}$, $\boldsymbol{K}_{eq}$, $\boldsymbol{K}_{eq\_reduced}$, $\boldsymbol{K}_{eq\_\phi\phi}$ and $\boldsymbol{K}_{eq\_\psi\psi}$.

4.1 Simply supported FGM plate

Frequency analysis of simply supported FG magneto-electro-elastic plate for different power-law index as n = 0, 1.0, 5.0 and 1000.0 has been carried out. The dimensions of the FGM plate are $L_x = L_y = 1$ m, $h = 0.3$ m.

Tables 1-4 show the results of frequency behavior of FGM plate by using present element and Bhangale's element [18]. Here, power-law index is n = 0 representing an isotropic plate with properties corresponding to that of homogeneous $BaTiO_3$ (piezoelectric) plate and n = 1000.0 corresponds to isotropic plate made up of magneto-electro-elastic material ($CoFe_2O_4$). Comparing with the results given by Bhangale, a good correlation is observed when applying the presented finite element.

Table 1. Normalized natural frequency for power-law index n = 0 of FGM plate

No.	f_{uu}	f_{eq}	$f_{eq\_reduced}$	$f_{\psi\psi}$	$f_{\phi\phi}$
1	1.8791(1.9180)	1.9100(2.1091)	1.9100(2.1091)	1.8791(1.9180)	1.9100(2.1091)
2	2.3020(2.3003)	2.3020(2.3003)	2.3020(2.3003)	2.3020(2.3003)	2.3020(2.3003)
3	2.4824(2.6503)	2.5225(2.8014)	2.5225(2.8014)	2.4824(2.6503)	2.5225(2.8014)
4	2.6330(2.8014)	2.7077(2.8153)	2.7077(2.8153)	2.6330(2.8014)	2.7077(2.8153)
5	3.5781(3.7772)	3.6373(3.9397)	3.6373(3.9397)	3.5781(3.7772)	3.6373(3.9397)

Table 2. Normalized natural frequency for power-law index n = 1 of FGM plate

No.	f_{uu}	f_{eq}	$f_{eq\_reduced}$	$f_{\psi\psi}$	$f_{\phi\phi}$
1	1.7383(1.8946)	1.7566(1.9897)	1.7566(1.9897)	1.7369(1.8901)	1.7577(1.9938)
2	2.1074(2.3394)	2.1077(2.3394)	2.1077(2.3394)	2.1074(2.3394)	2.1077(2.3394)
3	2.2488(2.6934)	2.2618(2.7800)	2.2617(2.7800)	2.2465(2.6925)	2.2640(2.7807)
4	2.4319(2.8170)	2.4659(2.8170)	2.4658(2.8170)	2.4301(2.8170)	2.4673(2.8170)
5	3.3852(3.8237)	3.4684(3.8905)	3.4679(3.8905)	3.3824(3.8231)	3.4699(3.8905)

Table 3. Normalized natural frequency for power-law index n = 5 of FGM plate

No.	f_{uu}	f_{eq}	$f_{eq\_reduced}$	$f_{\psi\psi}$	$f_{\phi\phi}$
1	1.6545(1.73467)	1.6613(1.74004)	1.6613(1.74004)	1.6532(1.72695)	1.6626(1.74769)
2	2.0092(2.20267)	2.0093(2.20267)	2.0093(2.20267)	2.0092(2.20267)	2.0093(2.20267)
3	2.1495(2.53548)	2.1533(2.54305)	2.1533(2.54305)	2.1479(2.53399)	2.1549(2.54447)
4	2.3026(2.60829)	2.3113(2.60829)	2.3113(2.60829)	2.3002(2.60829)	2.3136(2.60829)
5	3.2151(3.57426)	3.2352(3.57426)	3.2351(3.57426)	3.2100(3.57426)	3.2401(3.57426)

Table 4. Normalized natural frequency for power-law index n = 1000 of FGM plate

No.	f_{uu}	f_{eq}	$f_{eq\_reduced}$	$f_{\psi\psi}$	$f_{\phi\phi}$
1	1.5032(1.5477)	1.4989(1.5403)	1.4989(1.5403)	1.4989(1.5403)	1.5032(1.5477)
2	1.9763(1.9747)	1.9763(1.9747)	1.9763(1.9747)	1.9763(1.9747)	1.9763(1.9747)
3	2.1172(2.2607)	2.1153(2.2594)	2.1153(2.2594)	2.1153(2.2594)	2.1172(2.2607)
4	2.2461(2.3372)	2.2436(2.3372)	2.2436(2.3372)	2.2436(2.3372)	2.2461(2.3372)
5	2.9033(3.1866)	2.8996(3.1866)	2.8996(3.1866)	2.8996(3.1866)	2.9033(3.1866)

Note: Data format: results of present element / Bhangale's element [18]

From Tables 1–4 it is determined that as the value of power-law index increases, the natural frequency decreases as it is approaching toward the homogeneous magneto-electro-elastic material, which corresponds to n = 1000.0. This is due to the fact that piezoelectric effect has a tendency to increase the stiffness of the plate by induced electric field, while magnetostrictive material has a tendency to decrease the stiffness of the system by inducing the magnetic field. It is observed from Tables 1 and 4 that f_{eq} and f_{eq_reduce} classes of eigenvalues are the same; this is due to the fact that n = 0 represents the plate fully made up of $BaTiO_3$ only and n = 1000.0 corresponds to $CoFe_2O_4$ (magnetostrictive), where magneto-electro coupling coefficients are zero. In contrast, for n = 1.0 and 5.0, similar behavior is not observed for f_{eq} and f_{eq_reduce} classes of vibration in Tables 2-3. Further, it is observed that as power-law index n increases, the influence of the magnetic effect is more pronounced when compared to piezoelectric effect as the material approaches to homogeneous magnetostrictive. This is evidenced by looking at Tables 2-4.

4.2 Simply supported FG cylindrical shells

Studies have been carried out for FGM ($BaTiO_3$–$CoFe_2O_4$) cylindrical shells of radius r and thickness h. In present analysis it is assumed that the composition is varied from the inner to the outer surfaces, i.e., the inner surface of the shell is metal piezoelectric-rich, whereas the outer surface is magnetostrictive-rich. In addition, material properties are graded throughout the thickness direction according to the volume fraction power-law distribution. Fig. 1 provides the first axial mode frequency results associated with first 10 circumferential modes for a simply supported boundary condition obtained for different power law indexes for different r/h ratios. The influence of the power law index is mainly to change the magnitude of the first axial mode frequency. As the power law index increases the frequencies increase as well. This fact can be understood easily, as the elastic properties of magnetostrictive are higher compared frequencies associated with 10 circumferential harmonics for FGM cylindrical shells for different r/h ratios and power law index n to piezoelectric counterpart. The power law index does not have a great influence to alter the associated circumferential mode number to the lowest of the first axial mode frequency. However, the change in the r/h ratios of the FGM shell does shift the mode number of the lowest frequency. It is observed from Fig. 1, as r/h ratios increases the lowest frequency of the shells occurs at higher circumferential mode. This behavior is similar to conventional shells. It is also detected that the frequency does not vary much with r/h ratios for lower circumferential modes. This is also to be expected, as the membrane effect is more predominant at the lowest circumferential mode. As expected, at higher circumferential mode with the increase of r/h ratios the shell frequencies diminish and this is due to the fact that the bending stiffness reduces as r/h ratios increases. In addition it is also observed that as the r/h ratio increases the lowest circumferential mode is shifted.

5. Conclusions

In this paper, the frequency behavior of FG magneto-electro-elastic structures is studied for plates and shells having different volume fractions of $BaTiO_3$. The analysis is carried out using the proposed finite element formulation. The study established the following:

(a) The frequency characteristics of magneto-electro-elastic structure are similar to those of homogeneous isotropic structures.

(b) In general, the piezoelectric effect has the tendency of stiffening the plate and hence, increases the natural frequency of a structure. In contrast, pure magnetic effect has an inverse influence on the system frequency and reduces the structural natural frequency marginally.

© VIBROENGINEERING. JOURNAL OF VIBROENGINEERING. DECEMBER 2012. VOLUME 14, ISSUE 4. ISSN 1392-8716

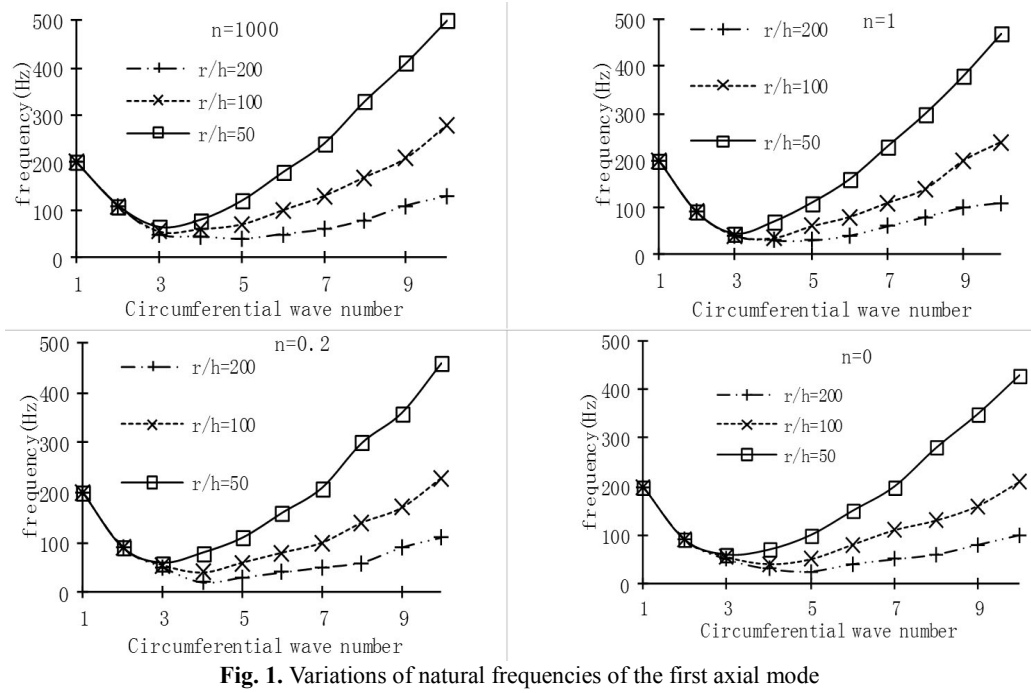

Fig. 1. Variations of natural frequencies of the first axial mode

(c) For FG magneto-electro-elastic structure, the volume fraction of $BaTiO_3$ in $BaTiO_3$-$CoFe_2O_4$ composite has considerable effect on the frequency of the system. As power-law index increases, the frequency decreases as the constituent of material reaches homogeneous magnetostrictive material for FGM plate model; the frequencies increases as exponential factor increases.

(d) While in the case of FGM shell model 'II', the influence of the power law index is mainly to change the magnitude of the first axial mode frequency. The power law index does not have a significant influence to alter the associated circumferential mode number to the lowest of the first axial mode frequency. However, the change in the thickness of the FGM shell does shift the mode number of the lowest frequency.

Acknowledgments

This research is supported by a grant from the Chinese Natural Science Foundation (No. 11172129, 50830201), and Jiangsu Colleges and Universities Superior Discipline Construction Project.

References

[1] **Pan E.** Exact solution for simply supported and multilayered magneto-electro-elastic plates. J. Appl. Mech, Vol. 68, Issue 4, 2001, p. 608–618.

[2] **Pan E., Heyliger P. R.** Free vibrations of simply supported and multilayered magneto-electro-elastic plates. Journal of Sound and Vibration, Vol. 252, Issue 3, 2002, p. 429–442.

[3] **Wang Yun, Xu Rongqiao, Ding Haojiang** et al., Three-dimensional exact solutions for free vibrations of simply supported magneto-electro-elastic cylindrical panels. International Journal of Engineering Science, Vol. 48, Issue 12, 2010, p. 1778–1796.

[4] **Zhong Xian-Ci, Lee Kang Yong** Dielectric crack problem for a magnetoelectroelastic strip with functionally graded properties. Arch. Appl. Mech., Vol. 82, Issue 6, 2012, p. 791–807.

[5] **Alberto Milazzo** An equivalent single-layer model for magnetoelectroelastic multilayered plate dynamics. Composite Structures, Vol. 94, Issue 6, 2012, p. 2078–2086.

[6] **Milazzo A., Orlando C.** An equivalent single-layer approach for free vibration analysis of smart laminated thick composite plates. Smart Mater. Struct., Vol. 21, Issue 7, 2012, p. 075031, (18 pages).

[7] **Buchanan G. R.** Layered versus multiphase magneto-electro-elastic composites. Composites Part B – Engineering, Vol. 35, Issue 5, 2004, p. 413–420.

[8] **Wang Jianguo, Qu Lei, Qian Feng** State vector approach of free-vibration analysis of magneto-electro-elastic hybrid laminated plates. Composite Structures, Vol. 92, Issue 6, 2010, p. 1318–1324.

[9] **Gülay Altay, M. Cengiz Dömeci** On the fundamental equations of electromagnetoelastic media in variational form with an application to shell laminae equations. International Journal of Solids and Structures, Vol. 47, Issue 3-4, 2010, p. 466–492.

[10] **Cao Xiaoshan, Shi Junping, Jin Feng** Lamb wave propagation in the functionally graded piezoelectric-piezomagnetic material plate. Acta Mech., Vol. 223, Issue 5, 2012, p. 1081–1091.

[11] **Wu Chih-Ping, Tsai Yi-Hwa** Dynamic responses of functionally graded magneto-electro-elastic shells with closed-circuit surface conditions using the method of multiple scales. European Journal of Mechanics A/Solids, Vol. 29, Issue 2, 2010, p. 166–181.

[12] **Pan E., Han F.** Exact solution for functionally graded and layered magneto-electro-elastic plates. International Journal of Engineering Science, Vol. 43, Issue 3-4, 2005, p. 321–339.

[13] **Huang D. J., Ding H. J., Chen W. Q.** Static analysis of anisotropic functionally graded magneto-electro-elastic beams subjected to arbitrary loading. European Journal of Mechanics A/Solids, Vol. 29, Issue 3, 2010, p. 356–369.

[14] **Bhangale R. K., Ganesan N.** Free vibration studies of simply supported non-homogeneous functionally graded magneto-electro-elastic finite cylindrical shells. Journal of Sound and Vibration, Vol. 288, Issue 1-2, 2005, p. 412–422.

[15] **Sze K. Y., Yao L. Q.** Modeling smart structures with segmented piezoelectric sensors and actuators. Journal of Sound and Vibration, Vol. 235, Issue 3, 2000, p. 495–520.

[16] **Zheng S. J.** Finite element simulation of wireless structural vibration control with photostrictive actuators. Science China – Technological Sciences, Vol. 55, Issue 3, 2012, p.709–716.

[17] **Jacob Aboudi** Micromechanical analysis of fully coupled electro-magneto-thermo-elastic multiphase composites. Smart Mater. Struct., Vol. 10, Issue 5, 2001, p. 867–877.

[18] **Bhangale R. K., Ganesan N.** Free vibration of simply supported functionally graded and layered magneto-electro-elastic plates by finite element method. Journal of Sound and Vibration, Vol. 294, Issue 4-5, 2006, p. 1016–1038.